A Rational Approach to the Design of Selective Substrates and Potent Nontransportable Inhibitors of the Excitatory Amino Acid Transporter EAAC1 (EAAT3). New Glutamate and Aspartate Analogues as Potential Neuroprotective Agents

Giuseppe Campiani,*,† Meri De Angelis,‡ Silvia Armaroli,‡ Caterina Fattorusso,‖ Bruno Catalanotti,† Anna Ramunno,† Vito Nacci,‡ Ettore Novellino,‖ Christof Grewer,§ Diana Ionescu,§ Thomas Rauen,# Roger Griffiths,⊥ Colin Sinclair,⊥ Elena Fumagalli,¥ and Tiziana Mennini¥

Dipartimento di Scienze Farmaceutiche, Universita' degli Studi di Salerno, via Ponte Don Melillo 11, 84084 Fisciano, Italy, Dipartimento Farmaco Chimico Tecnologico, Universita' degli Studi di Siena, via Aldo Moro, 53100 Siena, Italy, Dipartimento di Chimica delle Sostanze Naturali and Dipartimento di Chimica Farmaceutica e Tossicologica, Universita' degli Studi di Napoli "Federico II", via D. Montesano 49, 80131 Napoli, Italy, Max-Planck Institut fur Biophysik, Frankfurt/Main, Germany, Institute fur Biochemie, Westfalische-Wilhelms-Universitat Munster, Wihelm-Klemm-Str 2, D48149 Munster, Germany, Biomolecular Science Building, University of St. Andrews, St. Andrews, Fife KY16 9ST, Scotland, U.K., and Istituto di Ricerche Farmacologiche Mario Negri, via Eritrea 62, 20157 Milano Italy

Received February 5, 2001

Abstract: Two three-dimensional receptor interaction models for EAAT substrates and nontransportable inhibitors have been developed, and new glutamate (Glu) and aspartate (Asp) analogues have been synthesized. The analogues **1a** and **3** represent novel lead compounds for the development of EAAT substrates and nontransportable inhibitors, selective for EAATs over iGluRs, as possible neuroprotective agents useful to minimize the progression of chronic or acute neurodegenerative diseases. The role played by the protonatable amine function in the interaction with EAATs has been discussed.

Introduction. L-Glutamate (Glu) is the major excitatory neurotransmitter in the mammalian central nervous system (CNS). The process of excitatory neurotransmission is initiated by the presynaptic release of glutamate into the synaptic cleft, where glutamate activates ionotropic (iGluRs) and metabotropic (mGluRs) receptors, while the high affinity electrogenic transport systems (EAATs) contribute to the termination of the excitatory signal and to the recycling of the transmitter into the metabolic pool.[1−3] To date, five different mammalian subtypes of transporters have been cloned (EAAT1−5).[4] These Glu/Asp uptake systems are located at the pre- and postsynaptic levels in the CNS, in glial cells (EAAT1 and EAAT2), in the blood brain barrier (EAAT3),[5] and in the presynaptic vesicles.[6−8] The link between impairment of transporter functions and excitotoxic concentrations of Glu suggests that transporter dysfunction may contribute to neurodegenerative diseases.[4,9] It has been recently demonstrated that during ischemia the outward-activated glutamate transporter may be the major source of extracellular Glu.[10] Furthermore, under energy deprivation conditions, Glu can be released from glial cells by reversed transport.[11] Therefore, the design of "reversed transport inhibitors" (nontransportable inhibitors or blockers), with very low affinity for iGluRs, could represent a new strategy for the development of potential neuroprotective agents.[4] On the other hand, selective competitive substrates for EAATs, with negligible affinity for iGluRs, could represent a new therapeutic approach to minimize the progression of chronic neurodegenerative diseases involving glutamate toxicity.[4] In this Letter we describe a comprehensive approach, involving molecular modeling, synthesis, and biology in an attempt to discover such novel neuroprotective agents targeting EAATs. This approach led to the synthesis of new Glu and Asp analogues as selective high affinity substrates and nontransportable inhibitors, respectively. The Glu analogue **1a** and the Asp analogue **3** represent new prototypic compounds for the development of possible neuroprotective agents (Chart 1).

Chart 1. New EAAT Substrates (**1a**,**b** and **2**) and Inhibitors (**3**, **4**)

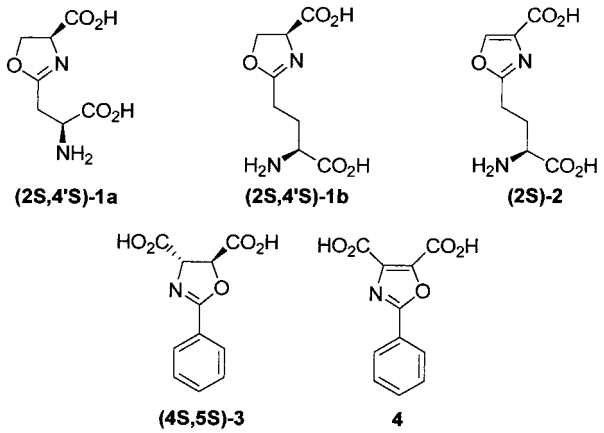

Molecular Modeling Studies. To design new and potent EAAT ligands, we investigated the conformational and structural features of known substrates (L-*threo*-3-OHAsp; L-*threo*-4-OHGlu, L-*trans*-2,4-PDC, *cis*-ACBD; L-CCGIII; 2,4MPDC) and nontransported inhibitors (L-*anti*-*endo*-3,4-MPDC; L-*trans*-2,3-PDC; L-*threo*-3-BnOAsp; kainic acid; dihydrokainic acid; L-*threo*-3-BzAsp).[12] By a combination of systematic conformational search (SYBYL, Tripos)[13] and energy minimization methods (cvff force fields; Discover, MSI),[14] we have generated hypothetical binding modes for competitive substrates and nontransportable inhibitors (Figure 1). This study allowed the definition of those structural and conformational parameters required for an EAAT ligand

* To whom correspondence should be addressed (Dipartimento di Scienze Farmaceutiche, Universita' degli Studi di Salerno, via Ponte Don Melillo 11/C, 84084 Fisciano, Salerno, Italy; tel 0039-089-964381; fax 0039-089-962828; e-mail campiani@unisa.it).
† Universita' degli Studi di Salerno.
‡ Universita' degli Studi di Siena.
‖ Universita' degli Studi di Napoli "Federico II".
§ Max-Planck Institut fur Biophysik.
# Westfalische-Wilhelms-Universitat Munster.
⊥ University of St. Andrews.
¥ Istituto di Ricerche Farmacologiche Mario Negri.

10.1021/jm015509z CCC: $20.00
Published on Web 07/12/2001

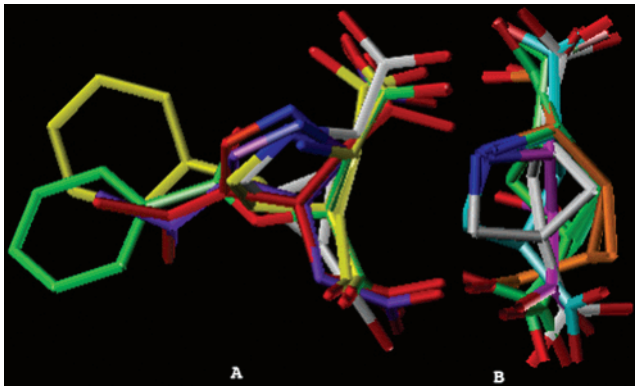

Figure 1. Superimposition of (A) nontransportable inhibitors—L-anti-*endo*-3,4-MPDC (white), l-*trans*-2,3-PDC (violet), L-*threo*-3-BnOAsp (yellow), kainic acid (redorange), dihydrokainic acid (purple), and L-*threo*-3-BzAsp (green)—and (B) competitive substrates—L-*threo*-3-OHAsp (magenta), L-*threo*-4-OHGlu (green-blue), L-*trans*-2,4-PDC (cyan), *cis*-ACBD (green), L-CCGIII (orange), and 2,4-MPDC (white). Superimposition was obtained by fitting the protonatable nitrogen (blue) and the two carboxylic carbons (oxygens in red). Hydrogens are omitted for clarity.

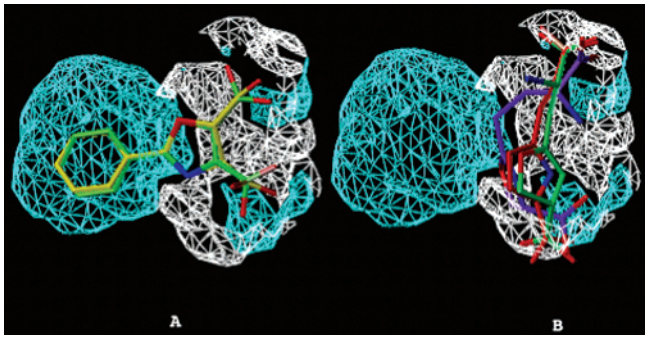

Figure 2. Fitting of newly designed blockers and substrates within the exceeding volume for blockers, with respect to substrates (cyan framework), and for substrates with respect to blockers (white framework). (A) New selective blockers: **3** (yellow), **4** (green). (B) New selective substrates **1a** (green-blue), **1b** (purple), **2** (red-orange). Superimposition was obtained by fitting the protonatable nitrogen (blue) and the two carboxylic carbons (oxygens in red). Hydrogens are omitted for clarity.

to behave as competitive substrate or blocker. The first evidence was that the calculated distances between the two carboxylic functions (see Table 1 in the Supporting Information) could not discriminate between substrates and nontransported inhibitors but between glutamate- and aspartate-related derivatives, which are present in both classes. Indeed, the main structural and conformational feature that can discriminate between substrates and blockers is the steric excess, as previously hypothesized.[12] From the superimpositions (Figure 1a,b) it can be observed that a constrained folded glutamate-like conformation (i.e., 2,3-PDC and 3,4-MPDC) forces the volume excess to occupy the edge opposite to the one where carboxylic groups are located (blockers), while a constrained unfolded glutamate-like conformation (i.e., 2,4-PDC and 2,4-MPDC) allows a quite uniform volume distribution on both sides of the backbone (Figure 2) (transportable substrates). On the other hand, the distance between the carboxylic groups represents a critical parameter responsible for improvement of selectivity toward Glu transporters, with respect to

Scheme 1. Synthesis of New EAAT Substrates[a]

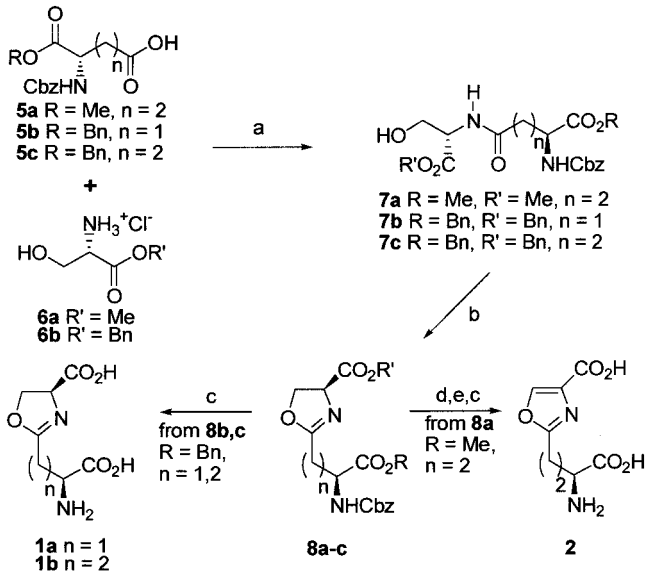

[a] (a) DCC, HOBT, TEA; (b) Burgess reagent; (c) H_2/Pd; (d) $BrCCl_3$, DBU; (e) LiOH, THF/H_2O, overnight.

Scheme 2. Synthesis of New EAAT Blockers[a]

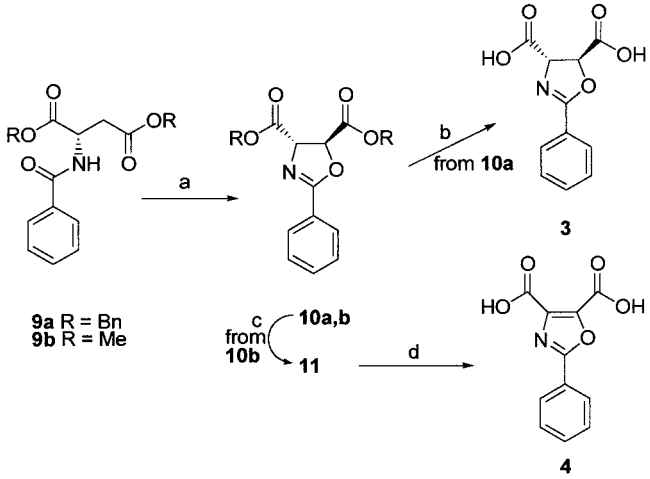

[a] (a) LHMDS, I_2, −78 °C; (b) H_2 (1 atm), Pd/C; (c) NiO_2; (d) LiOH, THF, H_2O.

iGluRs. Accordingly, we designed a new class of potentially selective molecules, predicted as competitive substrates (**1a**,**b** and **2**), based on an oxazoline or oxazole structure, bearing an alkyl chain as a flexible spacer between the two carboxylic functionalities (Chart 1A, Figure 2a), and the potentially selective EAATs blockers **3** and **4** (Chart 1A, Figure 2b) to investigate the importance of the protonatable function (critical for iGluRs interaction) for a selective binding to EAATs. Despite the lack of the free amine function (**3**, **4**), the designed inhibitors preserve a group capable to establish a hydrogen bonding interaction with the carrier, such as the heterocyclic oxygen/nitrogen atoms of **3** and **4**.

Chemistry. Synthesis of the new compounds was accomplished as shown in Schemes 1 and 2. By condensation of the α-methyl ester of N-Cbz L-glutamate **5a** and α-benzyl ester of N-Cbz L-aspartate (**5b**) or α-benzyl ester of N-Cbz L-glutamate (**5c**) with the hydrochloride salt of L-serine methyl and benzyl esters **6a**,**b**, the Ser-Glu **7a**,**c** and Ser-Asp **7b** dipeptidic compounds were obtained. We converted **7a**−**c** to the protected oxazoline

Table 1. K_i (μM) Values for Novel Glu and Asp Analogues for AMPA, Kainate, and NMDA Receptors[a]

compd	AMPA K_i	KA K_i	NMDA K_i
L-*threo*-3-OHAsp	NA	NA	0.49 ± 0.01
1a	NA	NA	NA
1b	103 ± 18	14 ± 0.6	9 ± 0.9
2	41 ± 5	8 ± 0.4	3 ± 0.7
3	NA	NA	NA
4	NA	NA	NA
L-Glu	1.1 ± 0.3	0.063 ± 0.007	0.2 ± 0.05

[a] Each value is the mean ± SEM of at least three separate experiments, performed in triplicate, and represents the concentration giving half-maximal inhibition of [^{3}H]AMPA (AMPA), [^{3}H]kainic acid (KA), and [^{3}H]CGP39653 (NMDA) binding to rat cortex homogenate. [b] NA = not active at $>10^{-4}$ M.

derivatives **8a**−**c** with Burgess reagent,[15] and then, after deprotection of the carboxylic and amine functions of **8b**,**c**, derivatives **1a**,**b** were obtained. Oxidation with $BrCCl_3$/DBU[16] of **8a** followed by deprotection provided the desired oxazole derivative **2**. In the case of blockers (Chart 1A), conversion of **9a** to the oxazoline derivative **10a**, by means of iodine and LHMDS,[17] followed by catalytic hydrogen-mediated deprotection afforded the oxazoline analogue **3**. Alternatively, nickel oxide oxidation[18a] of **10b**, in turn obtained from **10b**, provided the oxazole dimethyl ester **11**, which after saponification gave **4**.

In Vitro Pharmacology. In binding assays, all the compounds showed negligible affinity for the glycine site associated to NMDA receptor. The Asp analogues **3** and **4** showed negligible interaction with AMPA, kainate, and NMDA recognition sites (K_is $>10^{-4}$ M) (Table 1). Compound **1a**, which presents a longer distance between the two carboxylic groups with respect to Glu, did not show detectable inhibitory effect on [^{3}H]kainic acid, [^{3}H]AMPA, [^{3}H]MDL 105,519, and [^{3}H]CGP 39653 receptor binding (K_is $>10^{-4}$ M), while its superior homologues **1b** and **2** showed micromolar affinity for interaction with KA and NMDA receptors, whereas the affinity of these two compounds for AMPA receptors was in the high micromolar range (Table 1). Their relatively weak affinity for iGluRs could be explained on the basis of a favorable spatial arrangement of the longer alkyl chain.

Presumably, for **3** and **4**, the lack of a protonatable nitrogen (for oxazole and oxazoline rings, $pK_a = 0.8$ and 5.0, respectively[18b]) and the steric excess shown in the molecular modeling studies critically contribute to their EAAT selectivity. The whole set of compounds was subjected to electrophysiological studies. We used whole-cell current recordings from glutamate transporter-expressing mammalian cells as an assay for the biological activity of the new compounds.[7] According to the electrophysiological data, the new Glu and Asp analogues can be divided into two classes: (i) substrates that are transported by EAAC1 (**1a**,**b** and **2**) and (ii) nontransportable competitive inhibitors (**3** and **4**), as expected from the molecular modeling studies.

At saturating concentrations, the transported substrates evoked similar currents in EAAC1 as glutamate (Table 2, example trace for **2** shown in Figure 3A), suggesting that their steady-state transport rate does not differ significantly from that found for glutamate (~35 s^{-1} at V_m = 0 mV).[7] However, their apparent EAAC1 affinity varies in a range from 30 μM (**1a**) to 730 μM (**1b**), which is 100-fold greater than the apparent K_m of EAAC1 for glutamate (Table 2). These results suggest that the chain length as well as the configuration of the γ-carboxy-analogue group of the new substrates is important for their EAAC1 binding but not for the rate of transport. The nontransportable inhibitors **3** and **4** have two effects on the glutamate transporters: (i) they inhibit glutamate transport and (ii) they inhibit the leak-anion conductance in the absence of transported substrates, a behavior that is typical for competitive glutamate transporter inhibitors.[7] In the presence of 20 μM Glu, the Asp derivatives **3** and **4** inhibit EAAC1 in the micromolar concentration range (Table 2). In the absence of glutamate, the new blockers inhibited EAAC1 with a higher apparent affinity (Table 2, Figure 3C), in line with the competitive mechanism which was expected for such substances, as demonstrated in Figure 3C. The most potent and selective inhibitor for EAAC1 is **3** (examples of current recordings shown in Figure 3A), which exhibits an apparent inhibition constant of 14 ± 1 μM (Figure 3B). Interestingly, despite the lack of the protonatable free amine function, the oxazoline **3** retained significant affinity for EAAC1. Therefore, we conclude that protonation of the amino group is not necessary for high affinity interaction of the compound with EAAC1. In the absence of an electrochemical gradient for anions across the membrane, the new inhibitors do not induce any measurable current in EAAC1 (shown for **3** in the right panel of Figure 3A), indicating that they are, in fact, not transported by this glutamate transporter subtype. Furthermore, the excitotoxic effect on cerebellar granule cells of a subset of compounds was also evaluated. Cerebellar granule cells at 7-DIV were exposed for 24 h to increasing concentrations (0.1−1000 μM) of either L-glutamate, **1a**, and **3** (selective EAAC1 ligands) or **1b** and **2**, two EAAC1 substrates showing moderate affinity for iGluRs, before cell viability was monitored by the MTT assay. Glutamate exerted a concentration-dependent cytotoxic action in 7-DIV neurons (EC_{50} ~ 50 μM). In contrast, **1a**,**b**, **2**, and **3** were nontoxic in 7-DIV cells even after 24 h continuous exposure to concentrations up to 1 mM.

Table 2. Transport of the New Competitive Substrates **1a**,**b** and **2** by EAAC1 under Steady-State Conditions[a] and Inhibition of EAAC1 by **3** and **4** Compared to D,L-*threo*-3-BnOAsp under Steady-State Conditions in the Absence and Presence of L-Glutamic Acid[a]

compd	K_S (μM)	I_{max}/I_{max} (1 mM Glu)	K_i (μM) (no L-Glu)	I_{max}/I_{max} (1 mM Glu)	K_i (μM) (+20 μM L-Glu)
L-Glu	5.1 ± 0.2[b]	1			
1a	31 ± 6	1.15 ± 0.03			
1b	730 ± 60	0.92 ± 0.03			
2	100 ± 27	1.03 ± 0.10			
3			14 ± 1	−0.29 ± 0.1	42 ± 3 (68)[c]
4			75 ± 25	−0.25 ± 0.11	530 ± 60 (360)[c]
D,L-*threo*-3-OAsp			0.6 ± 0.1[b]	−0.24 ± 0.05[b]	4.9 ± 0.4 (3.5)[b,c,d]

[a] I_{max}/I_{max} (1 mM L-Glu) represents the fractional current induced by saturating concentrations of tested compounds compared to that induced by saturating concentrations of glutamate in the presence of intracellular SCN^-. [b] From ref 7. [c] The values in parentheses represent $K_i(S)$ calculated with eq 2 (Supporting Information), based on K_i (third column) and K_S = 5.1 μM. [d] 25 μM L-Glu.

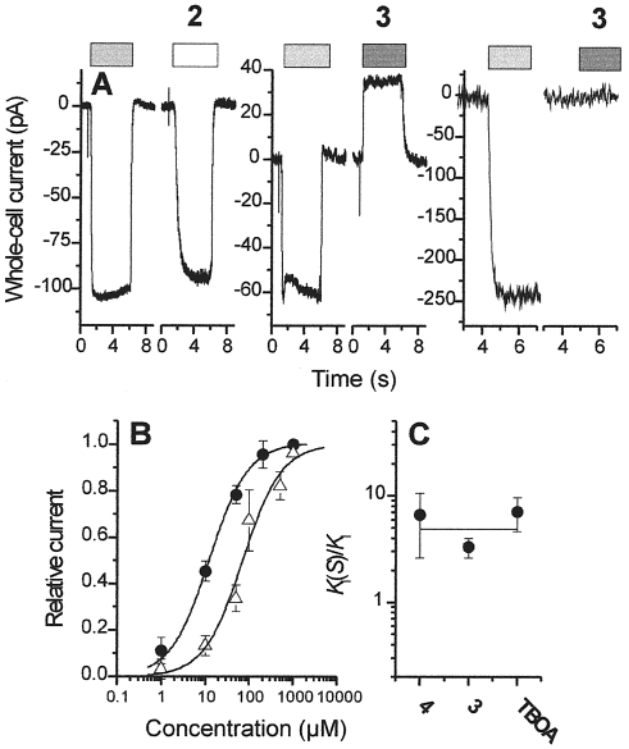

Figure 3. (A) Left panel: Compound **2** is a transported substrate of EAAC1. Whole-cell currents were evoked by application of 1 mM glutamate (light gray bar) or 1 mM **2** (white bar) (V_m = 0 mV, KSCN internal, pH 7.4, T = 22 °C). Similar results were obtained for **1a** and **1b** (not shown). Middle panel: Compound **3** generates an outward anion current. The experiment is similar to that shown in the left panel, but 200 μM **3** was applied (dark gray bar). The light gray bar indicates application of 10 μM glutamate. Right panel: Compound **3** is not transported by EAAC1. In the absence of an electrochemical gradient for anions ($[Cl^-]_i = [Cl^-]_o$, V_m = 0 mV), application of 1 mM **3** does not generate currents in EAAC1. (B): Dose−response relationships of EAAC1 outward currents generated by compounds **3** (closed circles) and **4** (triangles) in the absence of glutamate. (C): Inhibition of EAAC1 by Asp analogues **3** and **4** is competitive. The circles represent the ratio $K_i(S)/K_i$. $K_i(S)$ was determined at 20 μM glutamate. The line is the expected value of $K_i(S)/K_i$ calculated according to eq 2 (Supporting Information) for a competitive mechanism with K_S = 5.1 μM.

Conclusion. In summary, we disclosed the rational design of novel and potent glutamate and aspartate analogues selectively interacting with electrogenic glutamate transporters, as potent and selective EAAT substrates and nontransportable inhibitors. The new substrates (**1a**,**b** and **2**) described in this Letter potently interact with EAAC1, they are transported with the same turnover rate as Glu, and unlike all the other known substrates, they are characterized by weak-to-negligible affinity for iGluRs. On the other hand, this rational approach led to the identification of **3**, a potent and selective oxazoline-based blocker, the first characterized by the lack of a free amine function to be protonated at physiological pH, providing further insights on the role played by this function in the interaction with the EAAT binding site. Starting from our binding site interaction models and the new leads, these studies may pave the way for future rational design of selective EAAT substrates and nontransportable inhibitors as possible neuroprotective agents.

Acknowledgment. We thank the European Union for financial support (CEC BIOTECHNOLOGY PROGRAMME − Demostration Contract CT 98-0223). We are grateful to E. Bamberg for continuous encouragement and support and N. Watzke for help with the cell culture and transfection.

Supporting Information Available: Experimental details (chemistry, molecular modeling, and pharmacology (ref)), eqs 1 and 2, Table 1, and figures that portray the determination of Km values for EAAC1 substrates. This information is available free of charge via the Internet at http://pubs.acs.org.

References

(1) Michaelis, E. K. Molecular Biology of Glutamate Receptors in the Central Nervous System and Their Role in Excitotoxicity, Oxidative Stress and Aging. *Prog. Neurobiol.* **1998**, *54*, 369−415.
(2) Gegelashvili, G.; Schousboe, A. High Affinity Glutamate Transporters: Regulation of Expression and Activity. *Mol. Pharmacol.* **1997**, *52*, 6−15.
(3) Takahashi, M.; Billups, B.; Rossi, D.; Sorentis, M.; Hamann, M.; Attwell, D. The Role of Glutamate Transporters in Glutamate Homeostasis in the Brain. *J. Exp. Biol.* **1997**, *200*, 401−409.
(4) Seal, R. P.; Amara, S. G. Excitatory Amino Acid Transporters: A Family in Flux. *Annu. Rev. Pharmacol. Toxicol.* **1999**, *39*, 431−456 and references cited therein.
(5) O'Kane, R. L.; Martinez-Lopez, I.; DeJoseph, M. R.; Vina, J. R.; Hawkins, R. A. Na^+-dependent Glutamate Transporters EAAT1, EAAT2, and EAAT3 of the Blood-Brain Barrier. *J. Biol. Chem.* **1999**, *274*, 31891−31895.
(6) Takamori, S.; Rhee, J. S.; Rosenmund, C.; Jahn, R. Identification of a Vesicular Glutamate Transporter that Defines a Glutamatergic Phenotype in Neurons. *Nature* **2000**, *407*, 189−194.
(7) Grewer, C.; Watzke, N.; Wiessner, M.; Rauen, T. Glutamate Translocation of the Neuronal Glutamate Transporter EAAC1 Occurs within Milliseconds. *Proc. Natl. Acad. Sci. U.S.A.* **2000**, *97*, 9706−9711.
(8) Slotboom, D. J.; Konings, W. N.; Lolkema, J. S. Structural Features of the Glutamate Transporter Family. *Microbiol., & Mol. Biol. Rev.* **1999**, *63*, 293−307.
(9) Coyle, J. T.; Puttfarcken, P. Oxidative Stress, Glutamate, and Neurodegenerative Disorders. *Science* **1993**, *262*, 689−695.
(10) Rossi, D. J.; Oshima, T.; Attwell, D. Glutamate Release in Severe Brain Ischaemia is Mainly by Reversed Uptake. *Nature* **2000**, *403*, 316−321.
(11) Koch, H. P.; Chamberlin, A. R.; Bridges, R. J. Non Transportable Inhibitors Attenuate Reversal of Glutamate Uptake in Synaptosomes Following a Metabolic Insult. *Mol. Pharmacol.* **1999**, *55*, 1044−1048.
(12) Koch, H. P.; Kavanaugh, M. N. P.; Esslinger, C. S.; Zerangue, N.; Humphrey, J. M.; Amara, S. G.; Chamberlain, A. R.; Bridges, R. J. Differentiation of Substrates and Nonsubstrates Inhibitors of the High-Affinity, Sodium-Dependent Glutamate Transporters. *Mol. Pharmacol.* **1999**, *56*, 1095−1104.
(13) SYBYL Molecular Modeling System (version 6.6), Tripos Assoc., St. Louis, MO.
(14) Inight 98, Discover module, MSI, San Diego, CA.
(15) (a) Wipf P.; Xu W. Total Synthesis of the Antimitotic Marine Natural Product (+)-Curacin A. *J. Org. Chem.* **1996**, *61*, 6556−6562. (b) Wipf, P.; Miller, C. P. A Short, Stereospecific Synthesis of Dihydrooxazoles from Serine and Threonine Derivatives. *Tetrahedron Lett.* **1992**, *33*, 907−910.
(16) Williams, D. R.; Lowder, P. D.; Gu, Y.; Brooks, D. A. Studies of Mild Dehydrogenations in Heterocyclic Systems. *Tetrahedron Lett.* **1997**, *38*, 331−334.
(17) Cardillo, G.; Gentilucci, L.; Tolomelli, A.; Tomasini, C. A Practical Method for the Synthesis of −Amino −Hydroxy Acids. Synthesis of Enantiomerically Pure Hydroxyaspartic Acid and Isoserine. *Synth. Lett.* **1999**, *11*, 1727−1730.
(18) (a) Evans, D. L.; Minstewr, D. K.; Jordis, U. Nickel Peroxide Dehydrogenation of Oxygen-, Sulfur-, and Nitrogen- Containing Heterocycles. *J. Org. Chem.* **1979**, *44*, 497−501. (b) Oh, K. S.; Lee, C.-W.; Choi, S. H.; Lee, J. S.; Kim, K. S. Origin of the High Affinity and Selectivity of Novel Receptors for NH_4+ over K+: Charged Hydrogen Bonds vs Cation-p Interaction. *Org. Lett.* **2000**, *2*, 2679−2681.

JM015509Z